Pediatric Anesthesia 2009 **19** (Suppl. 1): 9–23 doi:10.1111/j.1460-9592.2009.03016.x

Review article

Imaging of the pediatric airway

HEDIEH K. ESLAMY MD AND BEVERLY NEWMAN MD
Lucille Packard Children's Hospital, Palo Alto, CA, USA

Summary

Airway compromise can be fixed, dynamic (with varying degrees of collapse during the respiratory cycle), or exhibit both components. The location of the abnormality can be classified as extrinsic (located outside but exerting mass effect on the airway) or intrinsic (intramural and/or intraluminal). The etiologies of airway compromise are categorized as: congenital, infectious, inflammatory, traumatic, vascular, or neoplastic (1). The role of imaging of the airway is to determine the presence, nature and anatomic level of airway compromise, categorize it as intrinsic or extrinsic, provide a differential diagnosis, and guide further imaging or management (1). The differential diagnosis of a lesion takes into account the patient's age and gender, location of the lesion, clinical presentation, and imaging appearance.

Keywords: airway; imaging; pediatric

Imaging methods

A systematic imaging approach to airway lesions begins with anteroposterior and lateral radiographs of the neck and/or chest, with additional imaging, if necessary, tailored to the clinical scenario and radiography findings. The pharynx, larynx, trachea, and central bronchi are seen as air-filled structures on radiographs. Abnormalities of the upper aerodigestive tract on the lateral neck radiograph may localize the process to the oral cavity, nasopharynx, oropharynx, hypopharynx, larynx or cervical trachea. Recognizing normal variations in the appearance of the airway in children is important, including expiratory buckling (2), deviation of the trachea away from the side of the aortic arch (usually to the right), and expiratory widening of retropharyngeal soft tissues (3) (Figure 1).

The high-kilovoltage, magnified, and filtered beam technique provides increased contrast resolution and demonstrates the airways better than conventional chest radiographs or fluoroscopy but is rarely used currently due to the easy availability of more detailed cross-sectional imaging techniques. Airway fluoroscopy is useful in suspected tracheobronchomalacia (Figure 2) as well as an endobronchial foreign body. Inspiratory-expiratory radiographs in a cooperative child or decubitus chest radiographs are often helpful when a foreign body is of concern (Figure 3) (4).

An esophagram may be helpful in cases of mediastinal lesions that impinge on the airway and esophagus including vascular rings and slings (Figure 4). However, this diagnosis can often be suspected from plain film radiographs and the esophagram does not provide the specific detailed anatomic delineation that is required for presurgical planning. Computed tomographic (CT) and magnetic resonance angiography (MRA) have largely replaced conventional angiography in providing this information.

Ultrasound (US) is an excellent imaging method for evaluating soft tissue abnormalities; it has the advantage of no radiation exposure and usually can be performed without sedation. CT of the head,

Correspondence to: Beverly Newman, 725 Welch Road, Department of Radiology, Room 1677, Palo Alto, CA 94304, USA (email: bevn@stanford.edu).

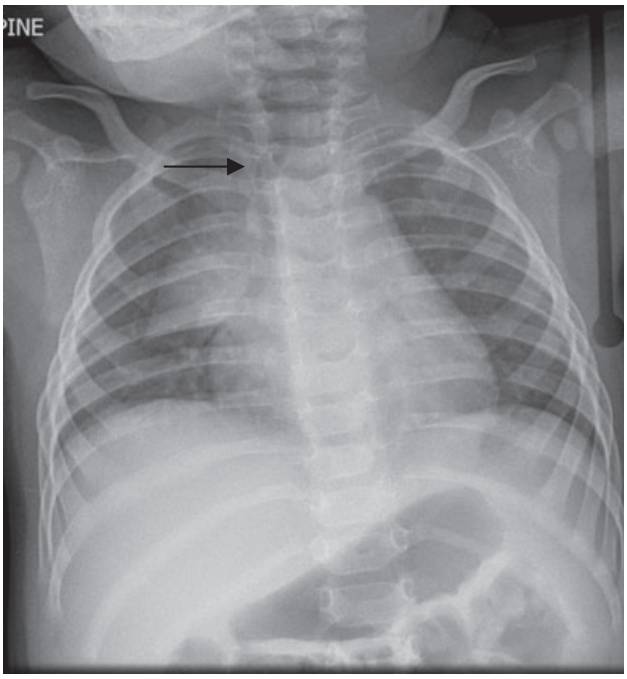

Figure 1
Frontal chest radiograph in a 10-month-old infant. Normal expiratory tracheal buckling to the right (arrow) is demonstrated. Note the prominent right thymic sail sign, also a normal variant.

neck, and chest is universally useful in providing global and detailed anatomy and depicting normal and abnormal soft tissue and bony structures, airways, vessels, and lung, and for identification of calcification. Magnetic resonance imaging (MRI) is useful for differentiation of soft tissues, including lymph nodes, muscles, vessels, thyroid, mediastinum, and chest wall. For the noninvasive assessment of the cervical and intrathoracic vessels, CT angiography (CTA) and MRA can provide exquisitely detailed images and can be reconstructed into a large variety of 2D and 3D displays to optimally assess anatomy and pathology. These include multiplanar, curved reformats, maximum and minimum intensity projections, and surface or volume rendered and virtual bronchoscopy reconstructions (1).

The radiation sensitivity of tissues especially thyroid and breast in infants and children should be considered in the choice of modality with US and MR preferred over CT when appropriate. When radiographs or CT are required the study should be tailored to minimize radiation to the neck organs and breast.

In addition to radiation exposure, adverse reactions to iodinated contrast media are a risk of contrasted CT studies, although the latter are extremely rare in children. However, CT has advantages over MR including much faster image acquisition; consequently sedation is required less often. CT also provides better spatial resolution and is less compromised in the presence of metallic devices. Lung parenchyma is much better visualized by CT. MR has the advantage of lack of ionizing radiation so that multiphase sequences e.g., angiographic can readily be obtained. Specific MR sequences provide detailed tissue specific (e.g., fat, fluid) information, but the studies are often very long. Contrast use for both CT

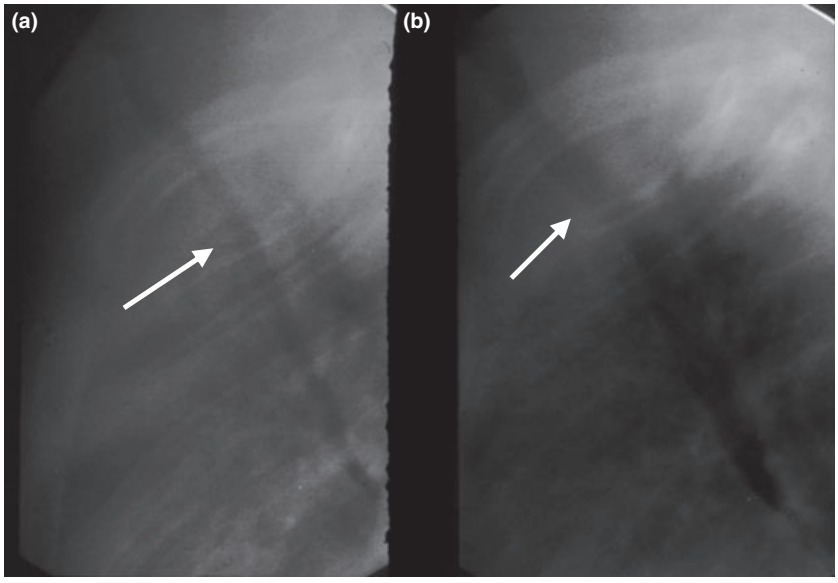

Figure 2
High kilovolt fluoroscopy in a 2.5-year-old child with intermittent noisy breathing demonstrates diffuse tracheomalacia with markedly decreased caliber of the airway in expiration (a) when compared with inspiration (b).

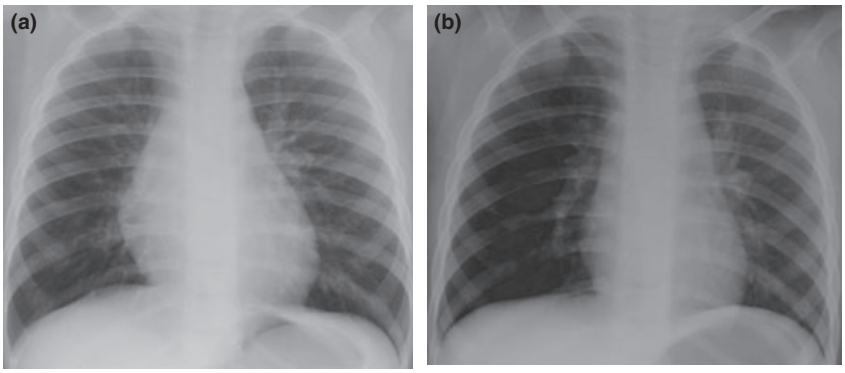

Figure 3
Two-year old with acute wheezing after eating peanuts. The inspiratory radiograph (a) demonstrates subtle hyperlucency on the right. The expiratory radiograph (b) confirms the suspicion of a right mainstem bronchus foreign body by demonstrating persistent expiratory air trapping and hyperlucency on the right with cardiomediastinal shift to the left. (Need permission to reproduce—Pediatric ER manual, editor Ewen Wang, Ha BoYoon, Newman B. Imaging of Pediatric Emergencies, Figure 5a and b, in press).

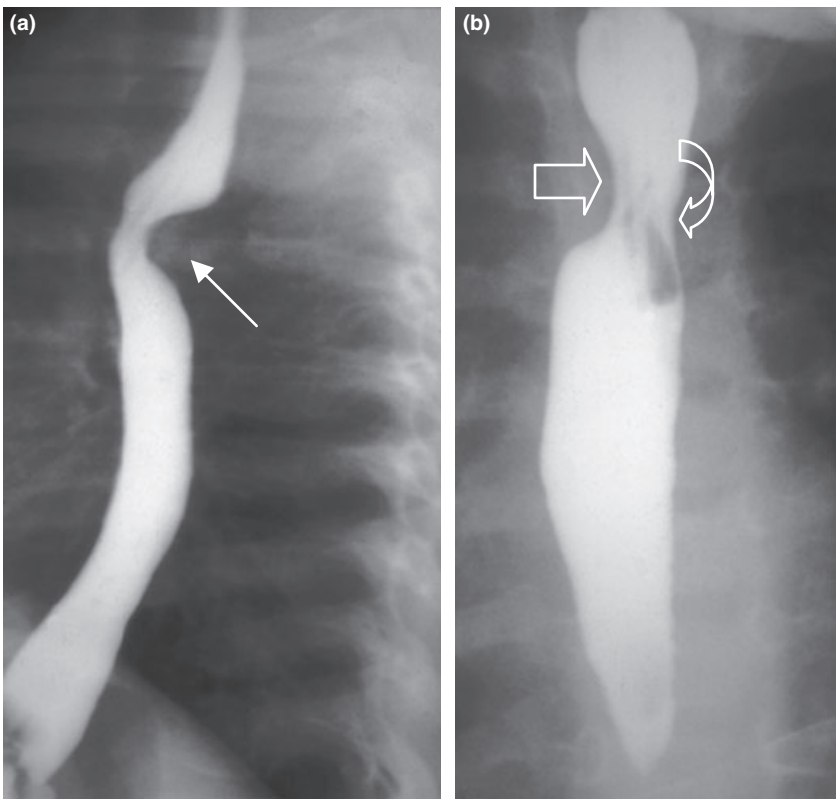

Figure 4
Lateral (a) and frontal (b) images from an esophagram in an 18-month-old child with recurrent respiratory symptoms show a large posterior esophageal indentation (arrow) and both right (block arrow) and left (curved arrow) lateral impressions on the esophagus from a double aortic arch vascular ring.

and MR should be carefully considered in patients with poor renal function with recent concern raised regarding nephrogenic systemic sclerosis, a debilitating diffuse skin condition, thought to be related to gadolinium contrast use, although very few cases have occurred in children (5).

Dynamic CT and MR imaging techniques are useful for evaluation of the airway in patients with suspected tracheobronchomalacia or dynamic airway compression. In cooperative children, CT images can be acquired during breath-holding at full inspiration and end expiration. In uncoopera-

tive children, CT images can be acquired at desired phases of respiration by the controlled-ventilation technique with sedation or anesthesia (6–8). Multiplanar and 3D volume-rendered image reconstructions further elucidate anatomic relationships. Hybrid positron emission tomography-CT imaging is used for staging, monitoring response to therapy, restaging, and surveillance of many head and neck and mediastinal tumors, especially lymphomas (9).

Extrathoracic (upper) airway lesions

As the differential diagnosis of airway lesions in neonates and children are somewhat different, they have been tabulated separately based on their anatomic location (Tables 1 and 2). Selected entities that affect the airways of neonates and children will be discussed and illustrated. Many lesions that affect the airway in the neonate may initially be suspected or diagnosed prenatally on fetal US and further characterized with fetal MRI to guide perinatal management (Figures 5 and 6) (14,15).

Congenital nasal airway obstruction occurs at three sites: piriform sinus aperture, midnose, and choanal airspace. The most common location for intrinsic congenital nasal airway obstruction is choanal atresia which may be bilateral or unilateral. The abnormality may be bony (Figure 7), bony and membranous, or purely membranous (uncommon) (16). A variety of space occupying lesions in the nasal cavity can cause airway obstruction (see Table 1, Figures 8 and 9) (11,17).

Normal adenoid tissues become visible on lateral radiographs of the nasopharynx between 3 and 6 months of age and are prominent throughout childhood (18). Grossly enlarged adenoids and palatine tonsils can produce narrowing of the nasopharyngeal airway (Figure 10) (19).

The most common laryngeal lesions causing inspiratory stridor in infants and children are laryngomalacia and vocal cord paralysis (20,21). In practice direct visualization (laryngoscopy) rather than indirect imaging (fluoroscopy) is utilized when evaluation other than clinical assessment is needed. Rare, congenital causes of airway symptoms in infants are atresias involving the pharynx or larynx (Figure 11) (22,23).

Table 1
Obstructive airway lesions in fetuses, neonates, and young infants

1. Nasal airway lesions
   1. Intrinsic lesions
      i. Piriform aperture stenosis
      ii. Midnose stenosis/hypoplasia
      iii. Choanal atresia
   2. Space occupying lesions
      i. Nasoencephalocele
      ii. Nasal glioma
      iii. Dermoid/epidermoid cyst
      iv. Hemangioma/lymphatic malformation
      v. Dacryocystocele and lacrimal duct cyst
      vi. Rhabdomyosarcoma
2. Head and neck lesions extrinsic to the airway
   1. Tumors: teratoma
   2. Malformations: lymphatic malformation, enteric duplication cyst, lingual-ectopic thyroid, thyroglossal duct cyst
   3. Mechanical obstruction of oro- or hypopharynx: macroglossia, micrognathia
   4. Iatrogenic: retropharyngeal perforation
   5. Large goiter: secondary to maternal goitrogen or antithyroid medication ingestion
3. Laryngeal abnormalities
   1. Laryngeal atresia
   2. Laryngomalacia
   3. Vocal cord paralysis
   4. Laryngeal cleft
   5. Laryngocele/web
4. Subglottic abnormalities
   1. Subglottic stenosis
      i. Congenital
      ii. Iatrogenic (intubation granulomas or acquired subglottic cysts)
   2. Subglottic hemangioma
5. Tracheal abnormalities
   1. Intrinsic lesions
      i. Agenesis
      ii. Stenosis
      iii. Tracheomalacia
      iv. Iatrogenic lesions: granulomas and stenosis
      v. Foreign body
   2. Extrinsic lesions
      i. Mediastinal masses
      ii. Cystic hygroma
      iii. Foregut malformations
      iv. Vascular abnormalities including rings and slings

Adapted from references (10) and (11).

There are four important infectious causes of acute upper respiratory obstruction in childhood: retropharyngeal abscess, acute viral laryngotracheobronchitis (croup), acute bacterial tracheitis (membranous croup), and epiglottitis. The diagnosis of epiglottitis is usually established clinically, although with the advent of *Hemophilus influenza* vaccination, this previously fairly common life threatening entity is uncommonly seen (24). If

Table 2
Obstructive airway lesions in children

Upper airway mucosal and submucosal abnormalities
1. Oral cavity
   1. Encroachment of tongue on airway
      i. Macroglossia: Beckwith-Wiedeman, hypothyroidism
      ii. Micrognathia: Pierre-Robin syndrome or cerebrocostomandibular syndrome
      iii. Hemangioma or venous/lymphatic malformation of tongue
      iv. Ectopic-lingual thyroid
   2. Other oral mass lesions
      i. Thyroglossal duct cyst
      ii. Dermoid cyst
      iii. Ranula
2. Nasopharynx/Oropharynx
   1. Adenoid/tonsillar inflammation
   2. Supraglotittis
   3. Foreign bodies
   4. Trauma
   5. Neoplasms
3. Retropharyngeal/parapharyngeal
   1. Phlegmon/abscess
   2. Hemorrhage/edema
   3. Lymphatic malformation
   4. Neoplasms

laryngeal and cervical tracheal abnormalities
1. Supraglottic abnormalities
   a. Laryngomalacia
   b. Epiglottitis
2. Glottic abnormalities
   a. Vocal cord paralysis
   b. Laryngeal cleft
   c. Recurrent respiratory papillomatosis
3. Subglottic abnormalities
   a. Croup
   b. Subglottic stenosis
      i. Congenital
      ii. Acquired (prolonged or traumatic intubation)
   c. Subglottic hemangioma
4. Other causes of airway narrowing
   a. Subacute/chronic esophageal foreign bodies
   b. Cervical tracheal foreign bodies
   c. Extrinsic compression of cervical trachea
      i. Benign: congenital cysts, hemangioma, lymphatic malformation
      ii. Neoplastic: teratoma, neuroblastoma

Central airway abnormalities—trachea and bronchi
1. Congenital anomalies of tracheobronchial tree
   a. Branching anomalies
      i. Bronchial atresia
      ii. Tracheoesophageal fistula
      iii. Bronchoesophageal fistula
      iv. Bronchobiliary fistula
      v. Tracheal bronchus
      vi. Bridging bronchus
      vii. Others: bilateral eparterial bronchi, bilateral hyparterial bronchi
   b. Congenital tracheal stenosis
   c. Abnormalities of dimension
      i. Tracheomegaly
      ii. Tracheomalacia: primary, secondary
      iii. Bronchomalacia
2. Extrinsic compression of the tracheobronchial tree
   a. Cardiac
      i. Large left atrium
      ii. Myocardiopathy
      iii. Tetralogy of Fallot/tetralogy of Fallot with absent pulmonary valve
      iv. Large left-to-right shunt
   b. Thoracic aorta
      i. Enlarged ascending aorta
      ii. Poststenotic aortic dilation
      iii. Midline position of descending aorta/midline descending aorta-carina compression syndrome
      iv. Right arch with left descending aorta
      v. Left arch with right descending aorta
      vi. Double arch
   c. Pulmonary vessels
      i. Enlarged pulmonary artery
      ii. Severe pulmonary hypertension
   d. Mediastinal masses/mass-like lesions
      i. Enteric cyst
      ii. Bronchogenic cyst
      iii. Infantile hemangioma
      iv. Lymphadenopathy
      v. Neoplasms: rhabdomyosarcomas, neurogenic tumors, germ cell tumors, thyroid neoplasms (rare)
      vi. Chronic esophageal foreign body
   e. Musculoskeletal
      i. Abnormal thoracic configuration
      ii. Kyphoscoliosis
      iii. Bone dysplasias
3. Acquired tracheobronchial abnormalities
   a. Postintubation tracheal stenosis
   b. Airway foreign bodies
4. Tracheobronchial neoplasms
   a. Tracheal neoplasms (rare)
   b. Bronchial neoplasms
      i. Adenomas: carcinoids, salivary gland tumors
      ii. Leiomyomas
      iii. Inflammatory pseudotumor

Adapted from references (1), (10), (12), and (13).

imaging is needed, a lateral radiograph should be performed in the upright position. Enlargement of the epiglottis and aryepiglottic folds is diagnostic (Figure 12a). Other causes of epiglottic enlargement are occasionally encountered including allergic anaphylaxis and ingestional or inhalational injury. Radiographic examination is often unnecessary in the classic case of viral croup (25), but may be valuable to exclude other causes of respiratory distress such as foreign body aspiration or epiglottitis. Anteroposterior radiographs of the neck are most suggestive of this diagnosis when

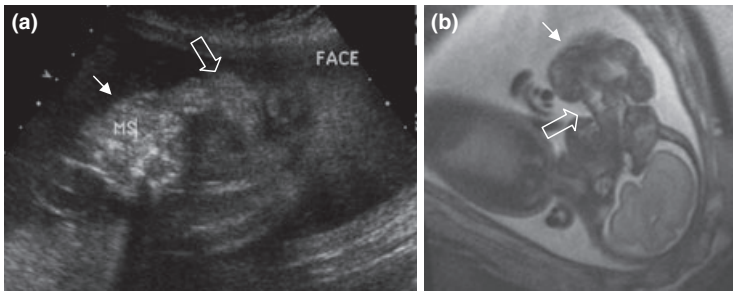

Figure 5
Oropharyngeal teratoma with airway obstruction in a fetus. Sagittal ultrasonography (a) and magnetic resonance imaging (b) in a 30-week fetus demonstrate an oropharyngeal mass (arrow) extruding from the mouth on a stalk (block arrows) and causing oropharyngeal obstruction. *Ex utero* intrapartum treatment was performed with resection of the mass in the delivery room at 32 weeks gestational age was performed due to oropharyngeal obstruction and inability to secure an airway.

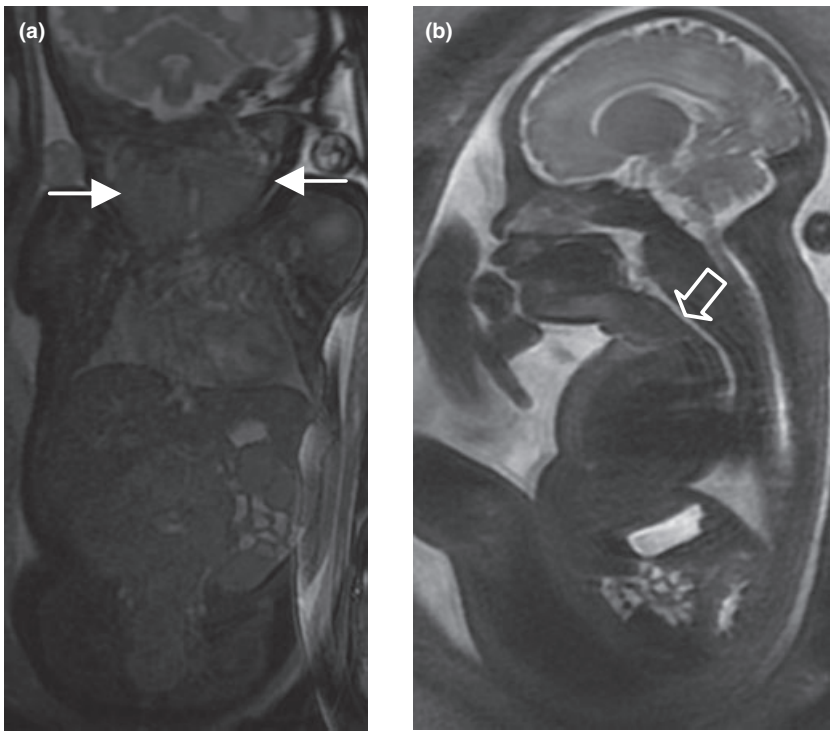

Figure 6
Goiter. Coronal (a) and sagittal (b) fetal magnetic resonance imaging (MRI) (T2 weighted) demonstrate a large goiter (arrows) with patent cervical trachea (block arrow) in a near term fetus whose mother was on propylthiouracil for Graves disease. Goiter was detected on obstetric ultrasonography and MRI was performed to evaluate cervical trachea patency and guide perinatal management.

there is symmetric narrowing of the tracheal air column for ≥5 to 10 mm below the level of the vocal cords (steeple sign) (Figure 12b). Membranous croup (acute bacterial tracheitis) has similar radiographic findings, but an inflammatory membrane may produce irregularity of the tracheal wall below the subglottic area (26–28).

Thickening of the retropharyngeal soft tissues may be due to inflammation/infection, abscess, edema or neoplasm (Figure 13). Retropharyngeal abscess can occur secondary to perforation of the hypopharynx (iatrogenic or due to trauma), but is most commonly due to suppuration of inflamed enlarged retrpharyngeal lymph nodes. The most common tumor in the retropharyngeal region is a lymphatic malformation (Figure 14) (29,30).

The normal subglottic airway in a neonate measures 5 to 7 mm in length. It is an area that is extremely vulnerable to trauma (intubation) and is the site of two specific congenital lesions, subglottic stenosis and subglottic hemangioma (Figure 15). The most common acquired subglottic

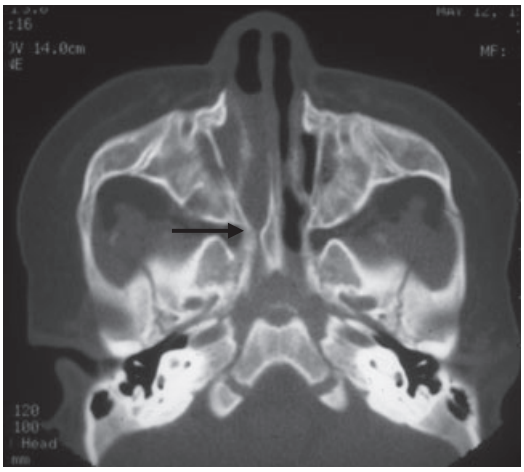

Figure 7
Right bony choanal atresia. Newborn infant with severe respiratory distress with feeding. The axial computerized tomography image demonstrates thickening of the posterior vomer and lateral nasal wall (arrows) with trapped fluid in the right nasal cavity.

lesions are intubation granulomas and acquired subglottic cysts (26).

Intrathoracic airway lesions

Tracheal agenesis (Figure 16) is a rare and usually lethal disorder, frequently associated with cardiopulmonary and other anomalies. Tracheal stenosis may be congenital or acquired; the latter is most often related to trauma from intubation. Congenital tracheal stenosis may be focal, diffuse, or funnel-shaped with complete cartilaginous rings lacking the normal posterior membranous portion (Figure 17). This is frequently associated with other anomalies including bronchial stenosis, tracheal bronchus, pulmonary sling, lung hypoplasia/agenesis, and tracheoesophageal fistula (31–34).

Tracheomalacia, focal or generalized narrowing of the airway during expiration due to cartilaginous collapse, occurs in both neonates and older children with variable symptomatology (Figure 2). The primary form is thought to be related to immaturity of the tracheobronchial cartilage whereas the secondary form is ascribed to external compression by a vascular anomaly or mass lesion (Figure 18). Fluoroscopy is the most practical method for dynamic imaging of the tracheal caliber through the respiratory cycle although in practice it is infrequently used. More often assessment is clinical or endoscopic with CT or MR employed when an extrinsic mass or vascular lesion is suspected (35,36).

Vascular rings may be associated with tracheal obstruction largely due to extrinsic airway compression and/or tracheomalacia but in the case of the pulmonary sling anomaly there may be associated long segment tracheal stenosis. The most common vascular rings are a double aortic arch (Figures 4 and 19) and a right aortic arch with an aberrant left subclavian artery and ligamentum arteriosum completing the ring. Plain chest radiographic findings that should raise concern for a vascular ring include leftward tracheal deviation due to a right aortic arch and anterior tracheal bowing on the lateral view. CTA or MRA provide complete evaluation of the vascular abnormalities and location and severity of

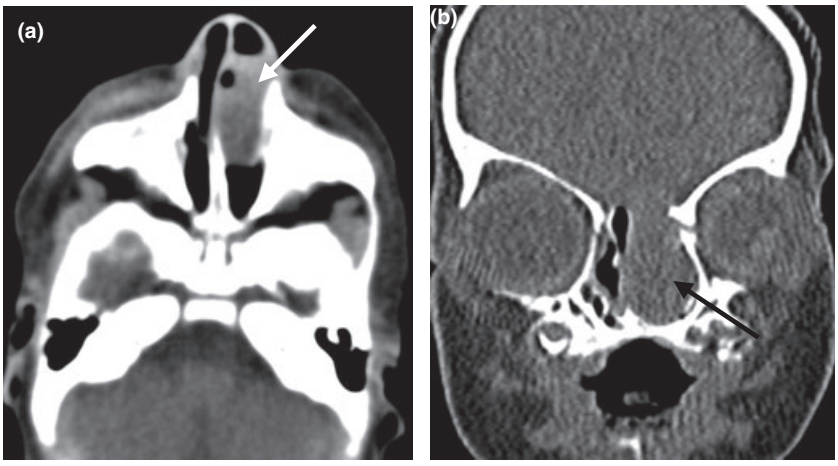

Figure 8
Nasal glioma. Axial (a) and coronal (b) computerized tomography images in a 1-day-old male show an expansile soft tissue mass (arrows) in the left nasal cavity.

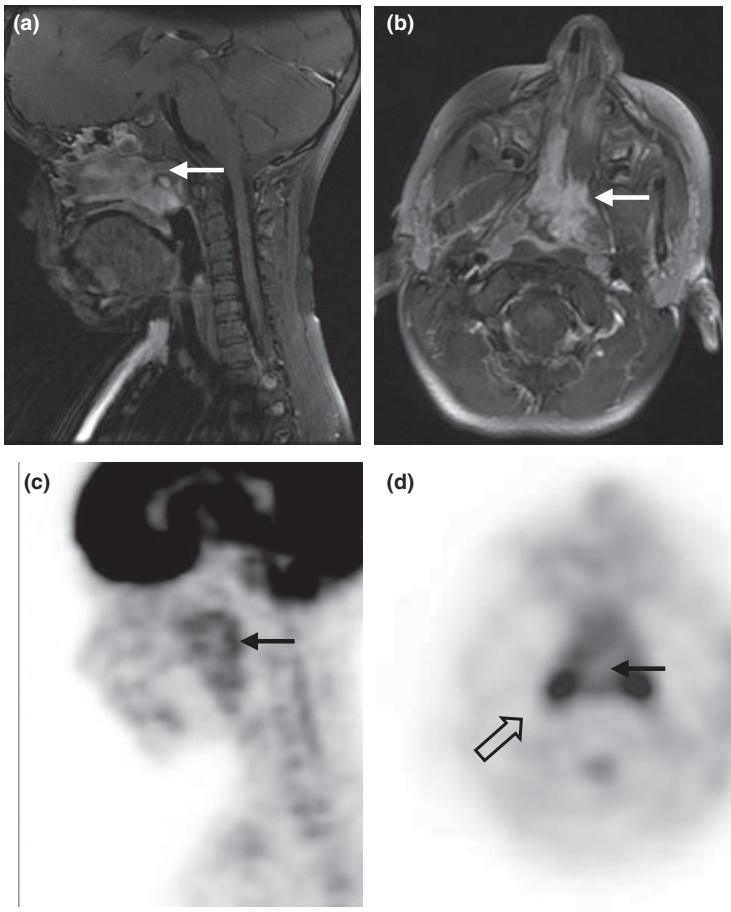

Figure 9
Embryonal rhabdomyosarcoma of the nasopharynx. Sagittal (a) and axial (b) T1-weighted magnetic resonance imaging images in a 5-year-old male with a heterogeneously enhancing mass in the nasopharynx extending into both nasal cavities (right more than left). Sagittal (c) and axial (d) F-18 FDG (flurodeoxyglucose) positron emission tomography images demonstrate a mildly hypermetabolic nasopharyngeal mass (arrows) with a standardized uptake value of 3. Note that the palatine tonsils (block arrow) demonstrate physiologic radiotracer uptake and are relatively more hypermetabolic than the neoplasm.

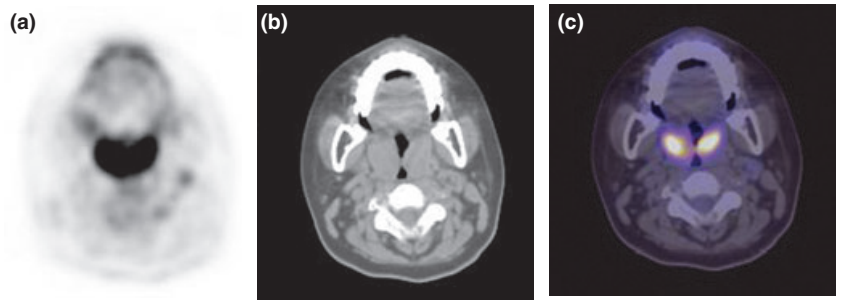

Figure 10
Physiologically enlarged palatine tonsils. Positron emission tomography (PET) (a), computerized tomography (CT) (b) and fused PET/CT images (c) in a 12-year-old boy with Hodgkin's lymphoma in remission demonstrate physiologically enlarged and hypermetabolic palatine tonsils.

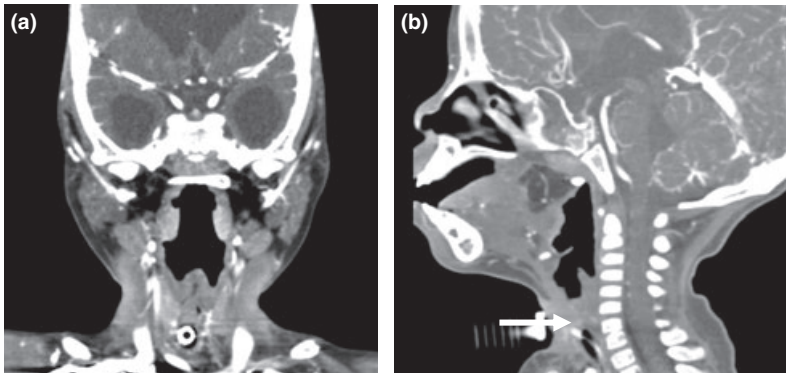

Figure 11
Oropharyngeal atresia. Coronal (a) and sagittal (b) computerized tomography images demonstrate lack of continuity of the pharyngeal air column with soft tissue interposed between the air in the oropharynx and trachea (arrow) at the level of the tracheostomy. The patient had difficulty breathing at birth and a tracheostomy was performed after unsuccessful attempts at intubation.

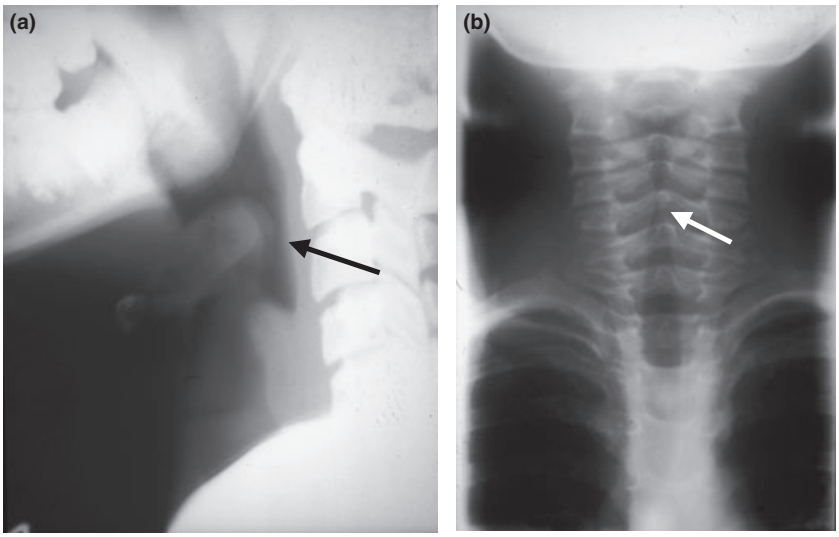

Figure 12
a) Epiglottitis. Lateral neck X-rays shows the enlarged thumb-like appearance of the swollen epiglottis (arrow) with thickening of the subjacent aryepiglottic folds. b) Croup. Note the steeple sign (arrow) with symmetric subglottic narrowing.

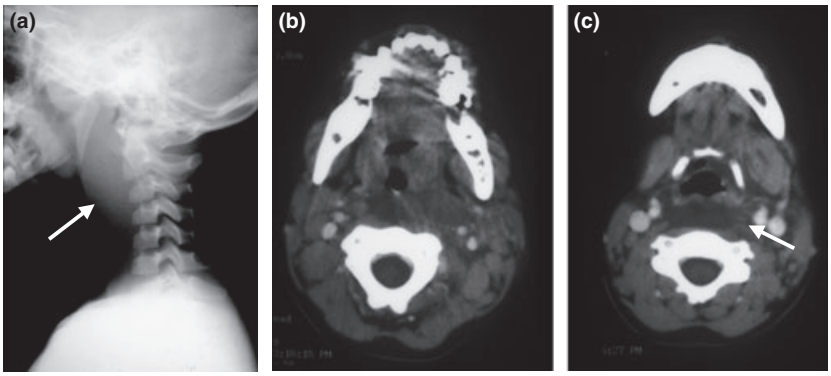

Figure 13
Retropharyngeal abscess. Two-year old with fever and drooling. The lateral radiograph of the neck (a) demonstrates widening and anterior bulging of the retropharyngeal soft tissues (arrow). On the contrast in computerized tomography images (b) a heterogeneous soft tissue mass with areas of low attenuation (fluid) is seen in the retropharyngeal space (arrow).

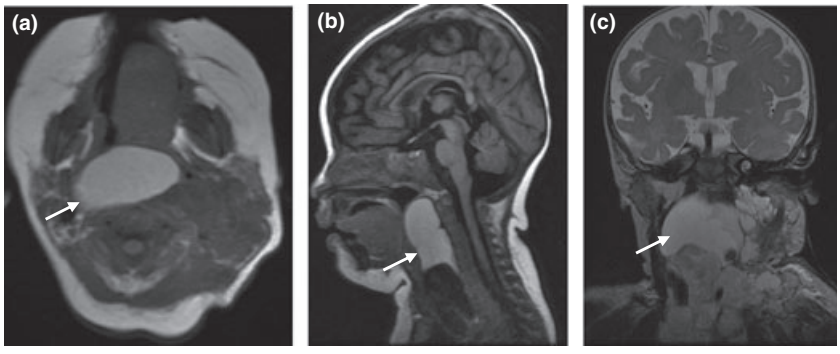

Figure 14
Retropharyngeal lymphatic malformation. Axial (a) and sagittal, (b) T1-weighted and coronal T2-weighted magnetic resonance images of the head and neck demonstrated a bright signal multicystic mass extending from the retropharyngeal space into the lateral neck and superior mediastinum (arrows). There is marked compression of the oropharynx and hypopharynx by the retropharyngeal component of the mass. The bright T1 and T2 weighted signal of the mass is typical of proteinaceous fluid such as lymph.

airway compression. Other vascular anomalies or enlarged cardiovascular structures may also cause airway compression (Table 2 and Figure 20) (37–42).

Abnormal airway branching patterns are summarized in Table 2 and may be associated with abnormalities of visceral and atrial situs. Patients with

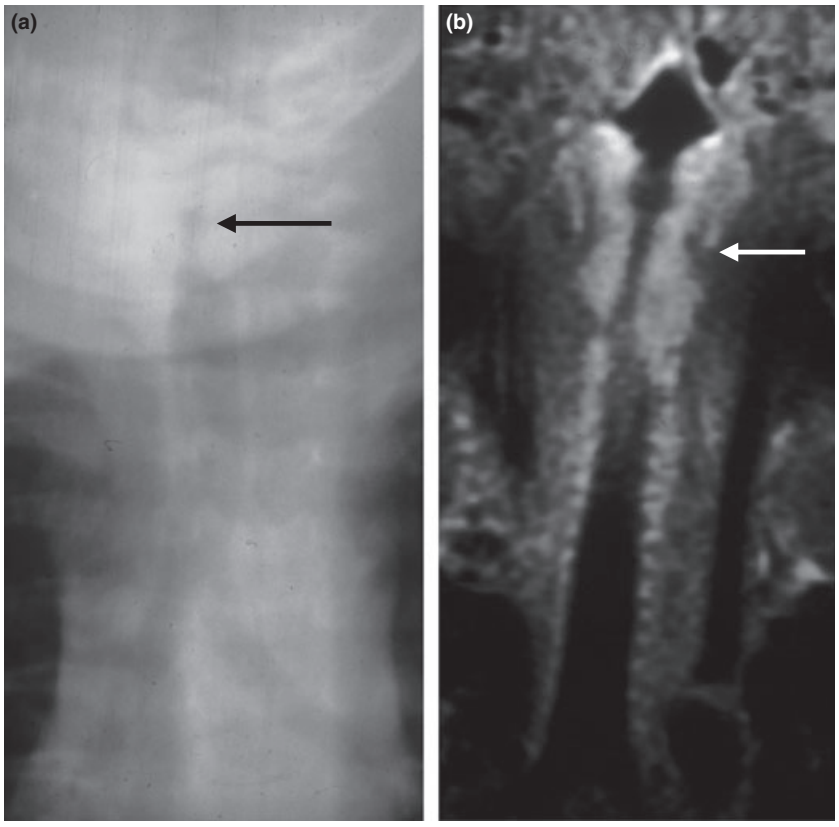

Figure 15
Subglottic hemangioma. One-year-old girl Frontal neck radiograph (a) demonstrates asymmetric left greater than right impingement on the subglottic airway (arrow). Coronal T1-weighted postcontrast magnetic resonance image demonstrates a discreet densely enhancing subglottic hemangioma surrounding the airway (arrow).

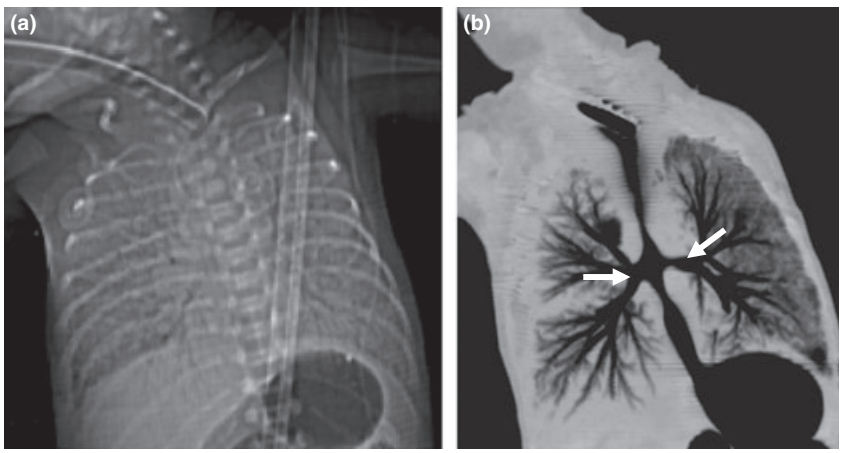

Figure 16
Tracheal agenesis with bilateral esophageal bronchi. Newborn infant presenting with severe respiratory distress and difficulty with intubation. The computerized tomography (CT) scout (a) demonstrates an endotracheal tube (ETT) with distal tip in the neck. Gaseous distention of the distal esophagus and stomach, poorly aerated lungs in conjunction with the clinical history suggest this may be an esophageal intubation. CT coronal minimum intensity projection image confirms an esophageal ETT, tracheal agenesis, and bilateral esophageal bronchi (arrows). [With kind permission from Springer Science and Business Media (32).]

asplenia (right isomerism) and polysplenia (left isomerism) syndromes have bilateral eparterial bronchi(short main stem bronchus superior to the pulmonary artery) and hyparterial bronchi (long main stem bronchus inferior to the pulmonary artery) respectively (Figure 21) (43,44).

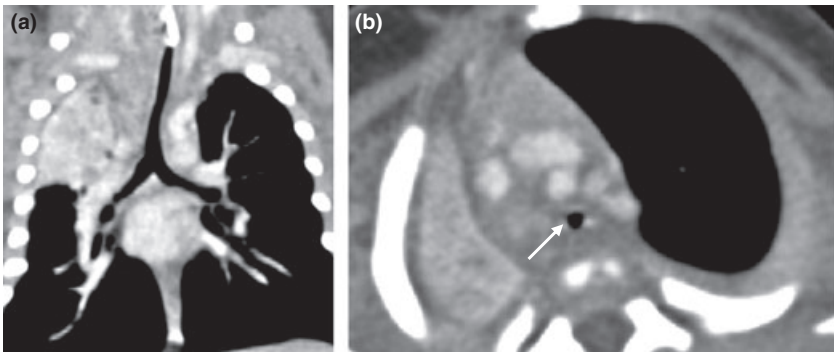

Figure 17
Severe diffuse tracheal stenosis. Four-day-old male with respiratory distress. Coronal (a) and axial (b) computerized tomography images demonstrate severe diffuse tracheal stenosis extending from the thoracic inlet to the mainstem bronchi with atelectasis of the right upper and middle lobes. Note the completely rounded configuration of the stenotic trachea on the axial image is suggestive of complete cartilaginous rings (arrow).

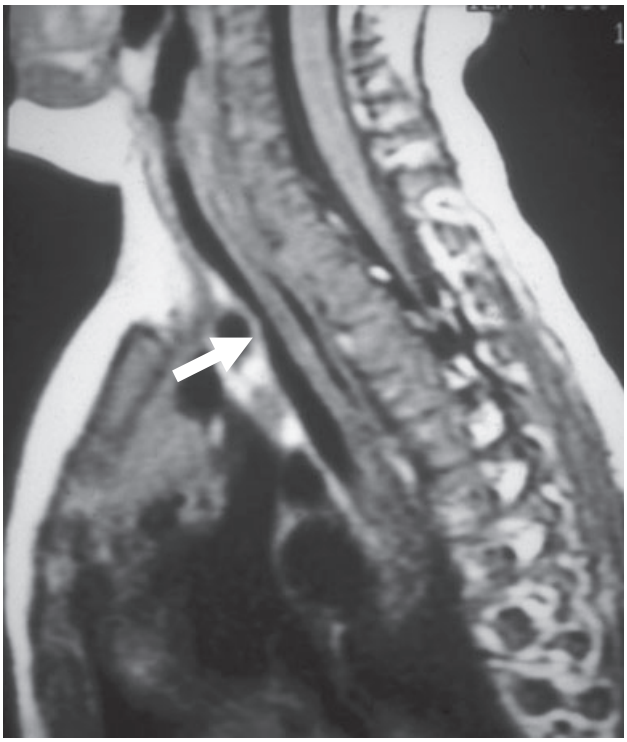

Figure 18
Tracheomalacia. Sagittal T1-weighted magnetic resonance image in an 11-month male with noisy breathing demonstrates innominate artery compressing the trachea (arrow) at the thoracic inlet.

Aspiration of a foreign body into the tracheobronchial tree is a common cause of respiratory distress in a child 6 months to 3 years old. In the presence of an airway foreign body there may be normal lung aeration, obstructive hyperinflation or obstructive atelectasis depending on the effect of the foreign body on the bronchial lumen and on the ingress and egress of air during inspiration and expiration. The physiologic negative pressure generated during inspiration causes the intrathoracic airways to normally be slightly larger on inspiration than expiration. Therefore when there is partial intrathoracic airway obstruction, the airway lumen collapses around the foreign body in expiration producing a 'ball valve effect' with obstructive hyperinflation. In obstructive atelectasis, ingress and egress of air are both blocked by the completely obstructing foreign body (45). Most foreign bodies lodge in a main stem bronchus, most are nonradiopaque and not directly visible, therefore inspiratory-expiratory films or lateral decubitus films should be obtained to detect air trapping in the affected lung. (Figure 3). CT is the most sensitive diagnostic imaging technique but is reserved for the diagnosis of elusive cases (Figure 22) (46–49).

Round foreign bodies such as a coin tend to lodge in the coronal plane in the esophagus and in the sagittal plane in the trachea (due to the posterior membranous tracheal wall) (Figure 23). Subacute or chronic esophageal foreign bodies may cause extrinsic tracheal compression secondary to the inflammatory response around the impacted foreign body (50,51). Mediastinal masses can compress the tracheobronchial tree. In early childhood, the most common mass adjacent to the airway is a bronchogenic cyst typically located in the mediastinum close to the carina (Figure 24) (52,53).

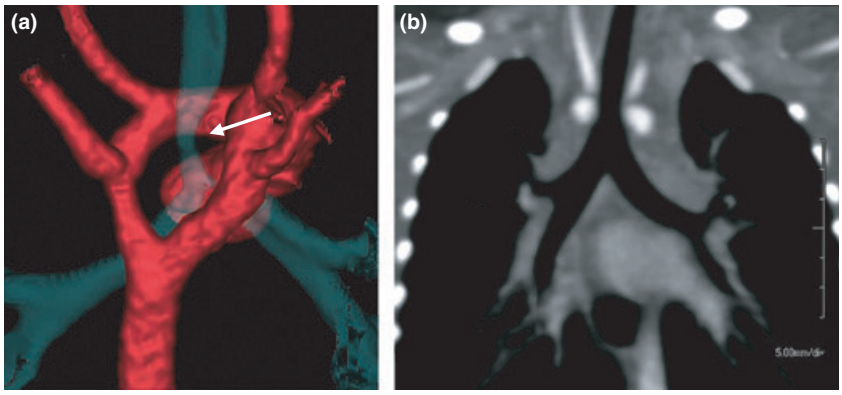

Figure 19
Double aortic arch with tracheal narrowing. Computerized tomography (CT) angiography with a volume rendered 3D image (a) and coronal MPR (Multi-Planar Reformatted) image (b) demonstrate a double aortic arch ring with moderate narrowing of the distal trachea (arrow) at the level of the bilateral arches in a 3-month-old female . (Images courtesy of Frandics Chan, MD, Stanford University).

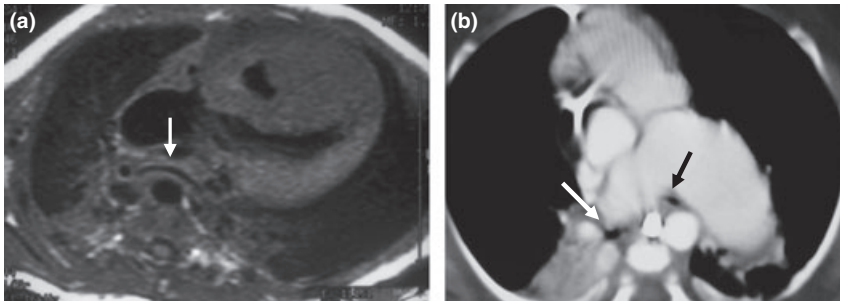

Figure 20
Compression of mainstem bronchi by vascular structures. a) T1 oblique axial magnetic resonance image in a 1-month-old infant with persistent wheezing demonstrates the prespinal location of the descending aorta (arrow) with bowing and narrowing of the adjacent left mainstem bronchus. [With kind permission from Springer Science and Business Media (57)]. b) Respiratory distress in a newborn infant with tetralogy of Fallot and absence of the pulmonary valve leaflets, a rare form of this cardiac lesion. A contrasted computerized tomography image demonstrates the aneurysmal central pulmonary arteries and tiny compressed mainstem bronchi (arrows).

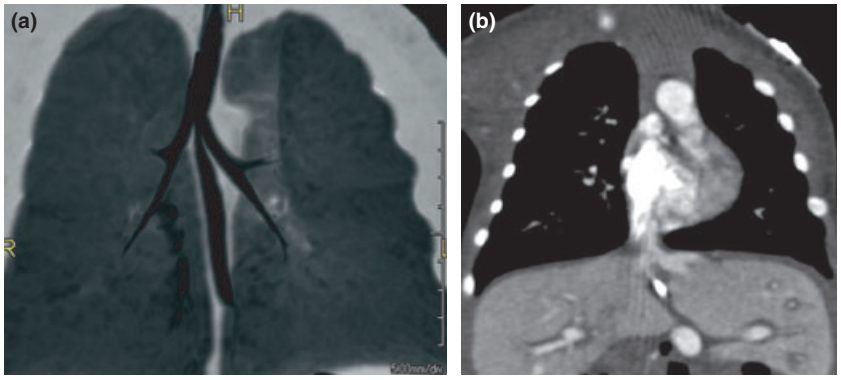

Figure 21
Asplenia and bilateral eparterial mainstem bronchi. Coronal minimum intensity projection image (a) and coronal computerized tomography slice demonstrate symmetric right-sided bronchial branching pattern bilaterally, midline liver, and absence of spleen in this newborn female infant with complex congenital heart disease.

Lymphoma is the most common childhood neoplasm to cause symptomatic airway compromise by extrinsic mass effect. (Figure 25) (54). Substantial narrowing of the trachea or major bronchi can occur without significant compromise of breathing at rest, and the caliber of the airway should be determined with radiography to evaluate the risk of life-threatening airway obstruction before any procedure requiring general anesthesia or heavy sedation (55,56). Even CT imaging must be approached carefully in these patients.

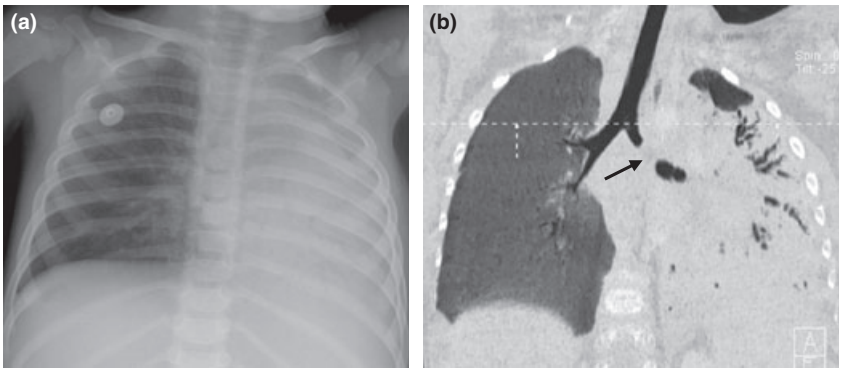

Figure 22
Bronchial foreign body. Eighteen-month-old male presenting with cough and shortness of breath for 2 weeks. The chest radiograph (a) demonstrates left lung atelectasis and ipsilateral cardiomediastinal shift. The minimum intensity projection computerized tomography image demonstrates focal obstruction of the mid left bronchus (arrow) with collapsed and consolidated left lung. Fragments of peanuts were removed from the bronchus endoscopically.

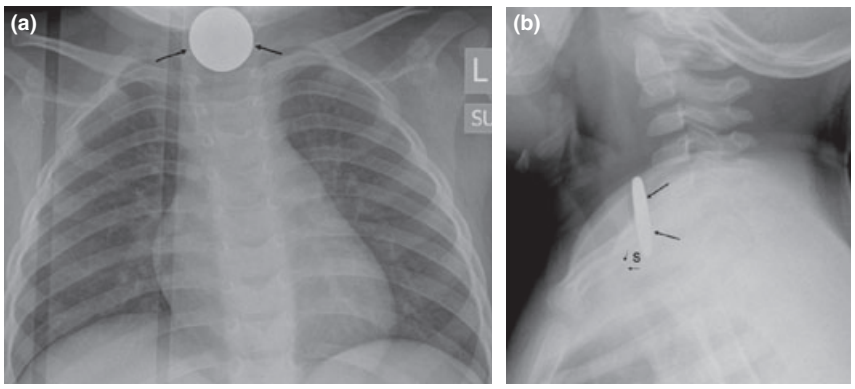

Figure 23
Subacute esophageal foreign body. Frontal (a) and lateral (b) chest X-rays in a 2 year old with a coin (arrows) in the esophagus. The adjacent narrowing of the airway and thickened tracheoesophageal soft tissues seen on the lateral view suggest this may be subacute in nature. (With kind permission from Cambridge Press. *Imaging of Pediatric Emergencies*, in press, Figures 6a and b).

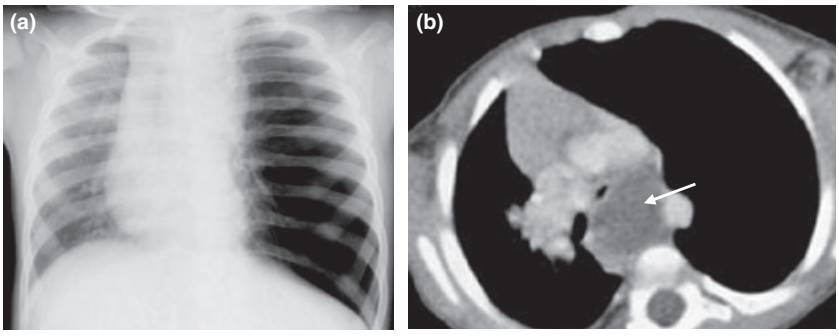

Figure 24
Bronchogenic cyst in 2 year old with 'asthma'. The frontal chest radiograph (a) shows marked air trapping in the left lung with contralateral shift. The axial contrasted computerized tomography image demonstrates the fluid-filled bronchogenic cyst (arrow) compressing the carina posteriorly and narrowing the left mainstem bronchus. (Need permission to reproduce—Chest imaging, *Rudolph's Textbook of Pediatrics Newman B*, in press, Figure 8a and b).

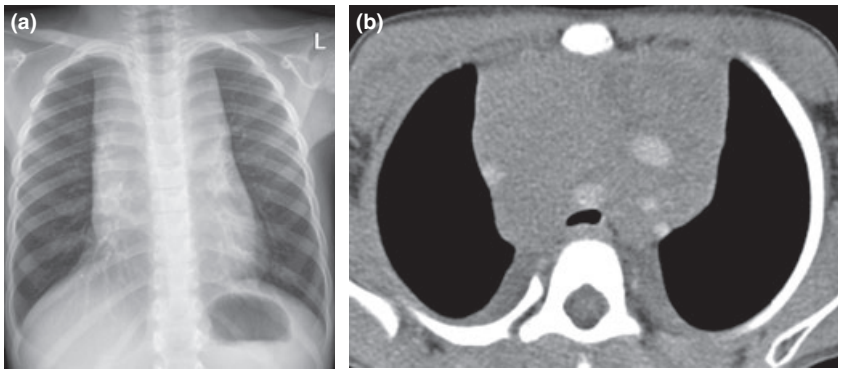

Figure 25
Mediastinal lymphoma. Eight-year-old boy presenting with a 2-week history of cough, wheezing, and shortness of breath (exacerbated in supine position). Frontal chest radiograph (a) demonstrates mediastinal widening. Contrasted computerized tomography (b) demonstrates an anterior mediastinal mass that encases the great vessels and narrows the trachea.

The above discussion is not intended to be exhaustive but rather selective of some of the more important and/or common conditions that affect the airway and how imaging may be used to evaluate these lesions. We have confined the discussion to the upper airway and central intrathoracic airways. Space does not permit inclusion of more peripheral airway lesions beyond the mainstem bronchi. Tables 1 and 2 shows in greater detail the causes of airway obstructive lesions in infants (Table 1) and children (Table 2).

Conflicts of interest

The authors have declared no conflicts of interest.

References

1 Yedururi S, Guillerman RP, Chung T *et al.* Multimodality imaging of tracheobronchial disorders in children. *Radiographics* 2008; **28:** e29. Review.
2 Chang LW, Lee FA, Gwinn JL. Normal lateral deviation of the trachea in infants and children. *Am J Roentgenol Radium Ther Nucl Med* 1970; **109:** 247–51.
3 Sneed WF, Miller RH, Mintz AA. Retropharyngeal pseudomasses. *South Med J* 1984; **77:** 528–30.
4 Capitanio MA, Kirkpatrick JA. The lateral decubitus film. An aid in determining air-trapping in children. *Radiology* 1972; **103:** 460–2.
5 Idée JM, Port M, Medina C *et al.* Possible involvement of gadolinium chelates in the pathophysiology of nephrogenic systemic fibrosis: a critical review. *Toxicology* 2008; **248:** 77–88. Review.
6 Lee EY, Mason KP, Zurakowski D *et al.* MDCT assessment of tracheomalacia in symptomatic infants with mediastinal aortic vascular anomalies: preliminary technical experience. *Pediatr Radiol* 2008; **38:** 82–8.
7 Goo HW, Kim HJ. Detection of air-trapping on inspiratory and expiratory phase images obtained by 0.3-second cine CT in the lungs of free-breathing young children. *Am J Roentgenol (AJR)* 2006; **187:** 1019–1023.
8 Long FR, Castile RG. Technique and clinical applications of full-inflation and end-expiration controlled-ventilation chest CT in infants and young children. *Pediatr Radiol* 2001; **31:** 413–422.
9 Jadvar H, Connolly LP, Fahey FH *et al.* PET and PET/CT in pediatric oncology. *Semin Nucl Med* 2007; **37:** 316–31. Review.
10 Bulas DI, Farmer DL. Prenatal diagnosis and treatment of the face, neck, and airway. In: Slovis TL, ed. *Caffey's Pediatric Diagnostic Imaging*, 11th edn. Philadelphia, PA: Mosby Elsevier, 2008: 37–72.
11 Slovis TL, Shore RM. Congenital anomalies and acquired lesions of the neonatal airway. In: Slovis TL, ed. *Caffey's Pediatric Diagnostic Imaging*, 11th edn. Philadelphia, PA: Mosby Elsevier, 2008: 1026–1077.
12 Cervantes LF, Medina LS, Effmann EL. Neck and upper airway. In: Slovis TL, ed. *Caffey's Pediatric Diagnostic Imaging*, 11th edn. Philadelphia, PA: Mosby Elsevier, 2008: 1086–1176.
13 Cohen RA, Kuhn JP. Larynx and cervical trachea. In: Slovis TL, ed. *Caffey's Pediatric Diagnostic Imaging*, 11th edn. Philadelphia, PA: Mosby Elsevier, 2008: 37–72, 1026–1077 and 1086–1176.
14 Effmann EL. Congenital lung malformations. In: Slovis TL, ed. *Caffey's Pediatric Diagnostic Imaging*, 11th edn. Philadelphia, PA: Mosby Elsevier, 2008: 37–72, 1026–1077 and 1086–1176.
15 Long FR, Druhan SM, Kuhn JP. Diseases of the bronchi and pulmonary aeration. In: Slovis TL, ed. *Caffey's Pediatric Diagnostic Imaging*, 11th edn. Philadelphia, PA: Mosby Elsevier, 2008: 37–72, 1026–1077 and 1086–1176.
16 Lowe LH, Booth TN, Joglar JM *et al.* Midface anomalies in children. *Radiographics* 2000; **20:** 907–922.
17 Donnelly LF, Strife JL, Bisset GS III. The spectrum of extrinsic lower airway compression in children: MR imaging. *AJR Am J Roentgenol* 1997; **168:** 59–62.
18 Narla LD, Newman B, Spottswood SS *et al.* Inflammatory pseudotumor. *Radiographics* 2003; **23:** 719–29.
19 Stevens GH, Schoot BC, Smets MJ *et al.* The ex utero intrapartum treatment (EXIT) procedure in fetal neck masses: a case report and review of the literature. *Eur J Obstet Gynecol Reprod Biol* 2002; **100:** 246–50. Review.

20 Levine D. Obstetric MRI. *J Magn Reson Imaging* 2006; **24:** 1–15. Review.
21 Slovis TL, Renfro B, Watts FB *et al.* Choanal atresia: precise CT evaluation. *Radiology* 1985; **155:** 345–8.
22 Barkovich AJ, Vandermarck P, Edwards MS *et al.* Congenital nasal masses: CT and MR imaging features in 16 cases. *AJNR Am J Neuroradiol* 1991; **12:** 105–16.
23 Jeans WD, Fernando DC, Maw AR. How should adenoidal enlargement be measured? A radiological study based on interobserver agreement *Clin Radiol* 1981; **32:** 337–40.
24 Macartney FJ, Panday J, Scott O. Cor pulmonale as a result of chronic nasopharyngeal obstruction due to hypertrophied tonsils and adenoids. *Arch Dis Child* 1969; **44:** 585–92.
25 McSwiney PF, Cavanagh NP, Languth P. Outcome in congenital stridor (laryngomalacia). *Arch Dis Child* 1977; **52:** 215–8.
26 Ross DA, Ward PH. Central vocal cord paralysis and paresis presenting as laryngeal stridor in children. *Laryngoscope* 1990; **100:** 10–3.
27 Al RA, Guven ES, Akturk Z *et al.* Prenatal diagnosis of isolated laryngeal atresia: case report and literature review. *J Ultrasound Med* 2007; **26:** 1243–9. Review.
28 Lee HC, O-Lee TJ, Madan A *et al.* Oropharyngeal atresia in a preterm infant: a case report and review of the literature. *Int J Pediatr Otorhinolaryngol* 2007; **71:** 1485–9. Review.
29 Mayo-Smith MF, Spinale JW, Donskey CJ *et al.* Acute epiglottitis. An 18-year experience in Rhode Island. *Chest* 1995; **108:** 1640–7.
30 Dawson KP, Steinberg A, Capaldi N. The lateral radiograph of neck in laryngo-tracheo-bronchitis (croup). *J Qual Clin Pract* 1994; **14:** 39–43.
31 John SD, Swischuk LE. Stridor and upper airway obstruction in infants and children. *Radiographics* 1992; **12:** 625–643.
32 Denneny JC III, Handler SD. Membranous laryngotracheobronchitis. *Pediatrics* 1982; **70:** 705–7.
33 Stroud RH, Friedman NR. An update on inflammatory disorders of the pediatric airway: epiglottitis, croup, and tracheitis. *Am J Otolaryngol* 2001; **22:** 268–275.
34 Craig FW, Schunk JE. Retropharyngeal abscess in children: clinical presentation, utility of imaging, and current management. *Pediatrics* 2003; **111**(6 Pt 1)**:** 1394–8.
35 Swischuk LE. Nasal passages, mandible, and the upper airway. In: Swischuk LE, ed. *Imaging of the Newborn, Infant and Young Child*, 5th edn. Philadelphia, PA: Lippincott Williams &Wilkins, 2004: pp. 173–222.
36 Sandu K, Monnier P. Congenital tracheal anomalies. *Otolaryngol Clin North Am* 2007; **40:** 193–217. viii. Review.
37 Strouse PJ, Newman B, Hernandez RJ *et al.* CT of tracheal agenesis. *Pediatr Radiol* 2006; **36:** 920–6.
38 Rovira J, Morales L, Rottermann M *et al.* Agenesis of the trachea. *J Pediatr Surg* 1989; **24:** 1126–7.
39 Berrocal T, Madrid C, Novo S *et al.* Congenital anomalies of the tracheobronchial tree, lung, and mediastinum: embryology, radiology, and pathology. *Radiographics* 2004; **24:** e17.
40 Berdon WE. Ring, sling, and other things: vascular compression of the infant trachea updated from the mid century to the millenium—the legacy of Robert E. Gross, MD, and Edward B. D. Neuchauser, MD. *Radiology* 2000; **216:** 624–632.
41 Lee KH, Lee KH, Yoon CS *et al.* Use of imaging for assessing anatomical relationships of tracheobronchial anomalies associated with left pulmonary artery sling. *Pediatr Radiol* 2001; **31:** 269–278.
42 Berdon WE, Baker DH. Vascular anomalies in the infant lung: rings, slings, and other things. *Semin Roentgenol* 1972; **7:** 39–47.
43 Backer CL, Ilbawi MN, Idriss FS *et al.* Vascular anomalies causing tracheoesophageal compression: review of experience in children. *J Thorac Cardiovasc Surg* 1989; **97:** 725–731.
44 Gomes AS, Lois JF, George B *et al.* Congenital anomalies of the aortic arch: MR imaging. *Radiology* 1987; **165:** 691–695.
45 Klinkhamer AC. Aberrant right subclavian artery: clinical and roentgenologic aspects. *AJR Am J Roentgenol* 1966; **97:** 438–446.
46 Schlesinger AE, Krishnamurthy R, Sena LM *et al.* Incomplete double aortic arch with atresia of the distal left arch: distinctive imaging appearance. *Am J Roentgenol (AJR)* 2005; **184:** 1634–1639.
47 Choo KS, Lee HD, Ban JE *et al.* Evaluation of obstructive airway lesions in complex congenital heart disease using composite volume-rendered images from multislice CT. *Pediatr Radiol* 2006; **36:** 219–223.
48 Cohen MS, Anderson RH, Cohen MI *et al.* Controversies, genetics, diagnostic assessment, and outcomes relating to the heterotaxy syndrome. *Cardiol Young* 2007; **17**(Suppl 2)**:** 29–43. Review.
49 Ghaye B, Szapiro D, Fanchamps JM *et al.* Congenital bronchial abnormalities revisited. *Radiographics* 2001; **21:** 105–19.
50 Oh KS, Newman B, Bowen AD *et al.* Pediatric airway disorders: practical approaches to imaging evaluation. *Curr Probl Diagn Radiol* 1989; **18:** 193–233. Review.
51 Blazer S, Naveh Y, Friedman A. Foreign body in the airway. A review of 200 cases. *Am J Dis Child* 1980; **134:** 68–71.
52 Linegar AG, von Oppell UO, Hegemann S *et al.* Tracheobronchial foreign bodies. Experience at Red Cross Children's Hospital, 1985–1990. *S Afr Med J* 1992; **82:** 164–7.
53 Swischuk LE. Acute respiratory distress with cyanosis. *Pediatr Emerg Care* 1987; **3:** 209–10.
54 Hong SJ, Goo HW, Roh JL. Utility of spiral and cine CT scans in pediatric patients suspected of aspirating radiolucent foreign bodies. *Otolaryngol Head Neck Surg* 2008; **138:** 576–80.
55 Smith PC, Swischuk LE, Fagan CJ. An elusive and often unsuspected cause of stridor or pneumonia (the esophageal foreign body). *Am J Roentgenol Radium Ther Nucl Med* 1974; **122:** 80–9.
56 Macpherson RI, Hill JG, Othersen HB *et al.* Esophageal foreign bodies in children: diagnosis, treatment, and complications. *AJR Am J Roentgenol* 1996; **166:** 919–24.
57 Newman B. Congenital bronchopulmonary foregut malformations: concepts and controversies. *Pediatr Radiol* 2006; **36:**773–91. Epub 2006 Mar 22. Review.
58 Winters WD, Effmann EL. Congenital masses of the lung: prenatal and postnatal imaging evaluation. *J Thorac Imaging* 2001; **16:** 196–206.
59 Glick RD, La Quaglia MP. Lymphomas of the anterior mediastinum. *Semin Pediatr Surg* 1999; **8:** 69–77.
60 Shamberger RC, Holzman RS, Griscom NT *et al.* Prospective evaluation by computed tomography and pulmonary function tests of children with mediastinal masses. *Surgery* 1995; **118:** 468–471.
61 Slinger P, Karsli C. Management of the patient with a large anterior mediastinal mass: recurring myths. *Curr Opin Anaesthesiol* 2007; **20:** 1–3.
62 Hungate R, Newan B *et al.* Left mainst bronchial narrowing: a vascular compression syndrome? Evaluation by magnetic resonance imaging. *Ped Radiology* 1998; **28:** 257–232.

Accepted 5 March 2009

